

Supplementary material for the article:

# Mainshock anticipated by intra-sequence ground deformations: insights from multiscale field and SAR interferometric measurements

Francesco Brozzetti <sup>1,2</sup>, Alessandro Cesare Mondini <sup>3</sup>, Cristina Pauselli <sup>2,4</sup>, Paolo Mancinelli <sup>4,5</sup>, Daniele Cirillo <sup>1,2,\*</sup>, Fausto Guzzetti <sup>3</sup>, Giusy Lavecchia <sup>1,2</sup>

<sup>1</sup> Dipartimento di Scienze Psicologiche, della Salute e del Territorio, Università G. d'Annunzio, via dei Vestini 31, 66100 Chieti, Italy; francesco.brozzetti@unich.it (F.B.); d.cirillo@unich.it (D.C.); glavecchia@unich.it (G.L.)

<sup>2</sup> Centro InterUniversitario per l'Analisi SismoTettonica tridimensionale (CRUST), Italy;

<sup>3</sup> Consiglio Nazionale delle Ricerche-Istituto di Ricerca per la Protezione Idrogeologica (CNR-IRPI), 06128 Perugia, Italy; alessandro.mondini@irpi.cnr.it (A.C.M.); fausto.guzzetti@irpi.cnr.it (F.G.)

<sup>4</sup> Dipartimento di Fisica e Geologia, Università degli Studi di Perugia, piazza dell'Università 1, 06123 Perugia, Italy; cristina.pauselli@unipg.it (C.P.)

<sup>5</sup> Dipartimento di Ingegneria e Geologia, Università G. d'Annunzio, via dei Vestini 31, 66100 Chieti, Italy; paolo.mancinelli@unich.it (P.M.)

\* Correspondence: d.cirillo@unich.it

This supplementary material consists of 5 figures and a supplementary methods section.

## Supplementary figures

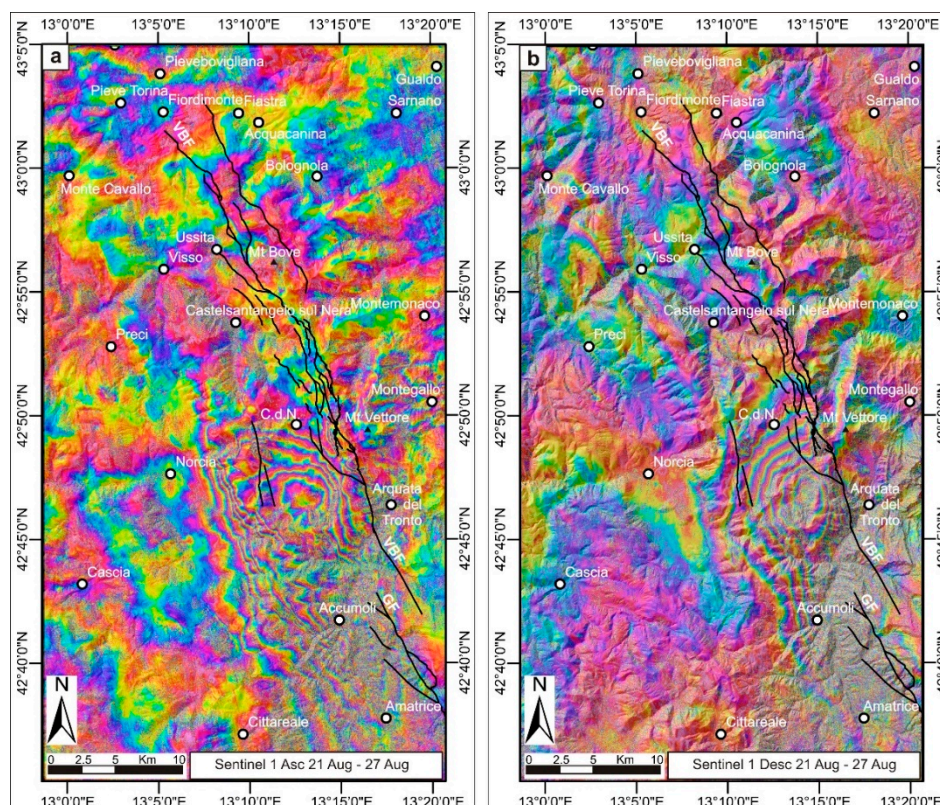


**Figure 1.** Coseismic interferograms for the 24 August, Mw 6.0 foreshock.

(a) Interferogram prepared using a pair of ESA Sentinel-1 images taken on 21 and 27 August 2016 along relative ascending orbit 117. (b) Interferogram prepared using a pair of ESA Sentinel-1 images taken on 21 and 27 August 2016 along relative descending orbit 22. The thick black lines show traces of the VBF. The colours show patterns of deformation around the Mt Vettore-Mt Bove Fault (VBF). One colour cycle corresponds to one interferometric fringe, ~ 2.8 cm along the satellite Line of Sight (LoS). We prepared the interferograms to compare the fringe pattern shown in the ESA's SEOM Programme InSARap project interferogram obtained using the same images (blue lines in Fig. 1a). C.d.N = Castelluccio di Norcia.

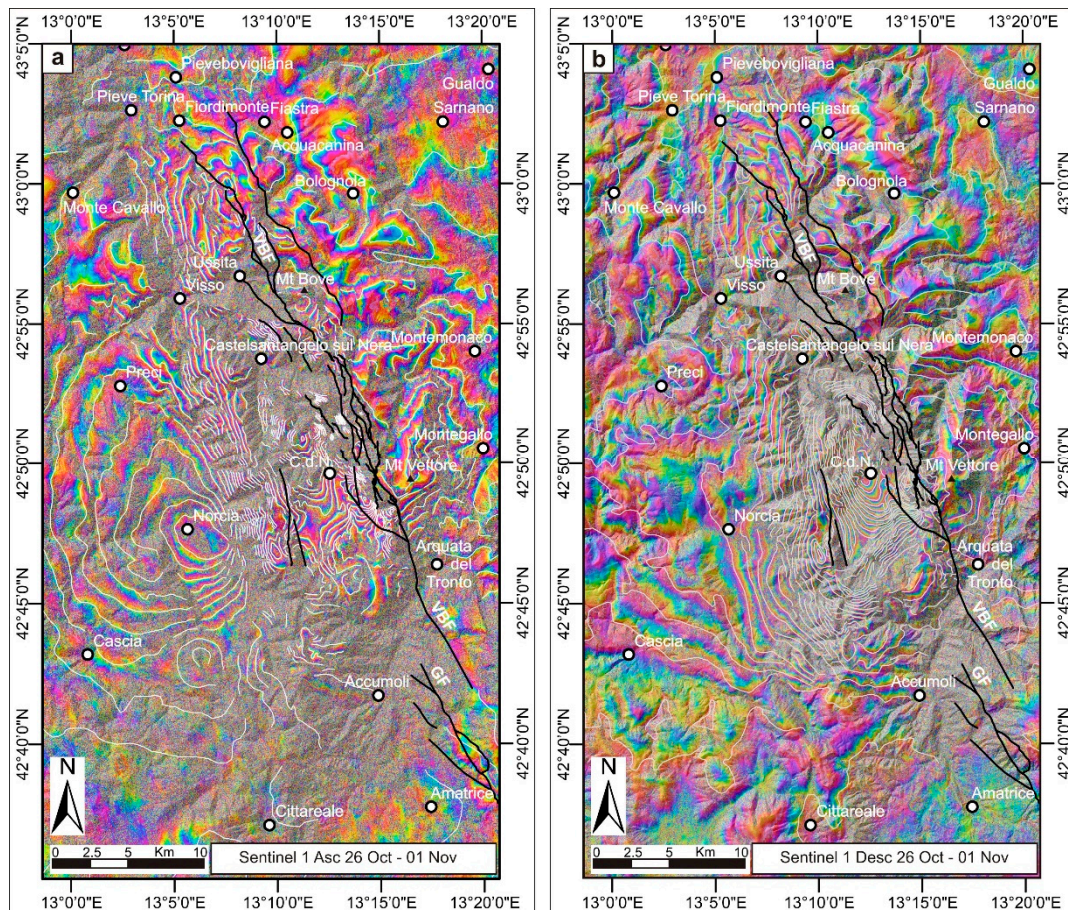


**Figure S2.** Coseismic interferograms cumulating the effects of the 26 October Mw 5.9 foreshock and 30 October Mw 6.5 mainshock.

(a) Interferogram prepared using a pair of ESA Sentinel-1 images taken on 26 October and 1 November 2016, along relative ascending orbit 117. (b) Interferogram prepared using a pair of ESA Sentinel-1 images taken on 26 October and 1 November 2016 along relative descending orbit 22. The thick black lines show the traces of the VBF. The colours show the patterns of deformation around the Mt Vettore–Mt Bove Fault (VBF). One colour cycle corresponds to one interferometric fringe,  $\sim 2.8$  cm along the satellite Line of Sight (LoS). We prepared the interferograms to compare the fringe pattern shown in the NERC Centre for Observation and Modelling of Earthquakes, Volcanoes and Tectonics, COMET interferogram obtained from ESA Sentinel-1 images acquired the 21 and 27 October 2016 along a descending relative orbit (green lines in Fig. 1a), and the fringe pattern shown in the ESA's SEOM Programme InSARap project interferogram obtained using images taken along ascending relative orbit 44 (black lines in Figure 1b).



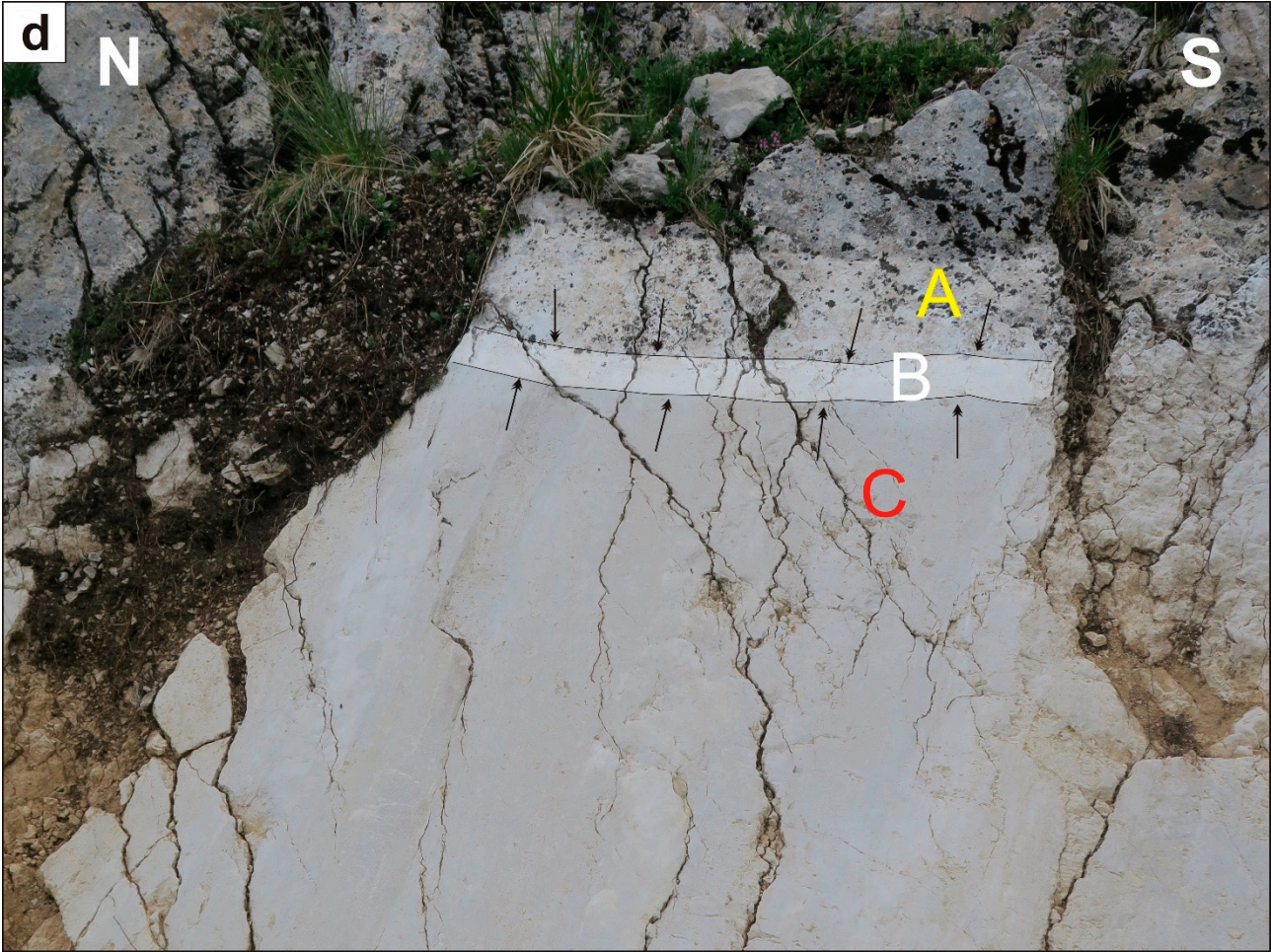
Supplementary Figure S3a



Supplementary Figure S3b



Supplementary Figure S3c



Supplementary Figure S3d



Supplementary Figure S3e



Supplementary Figure S3f

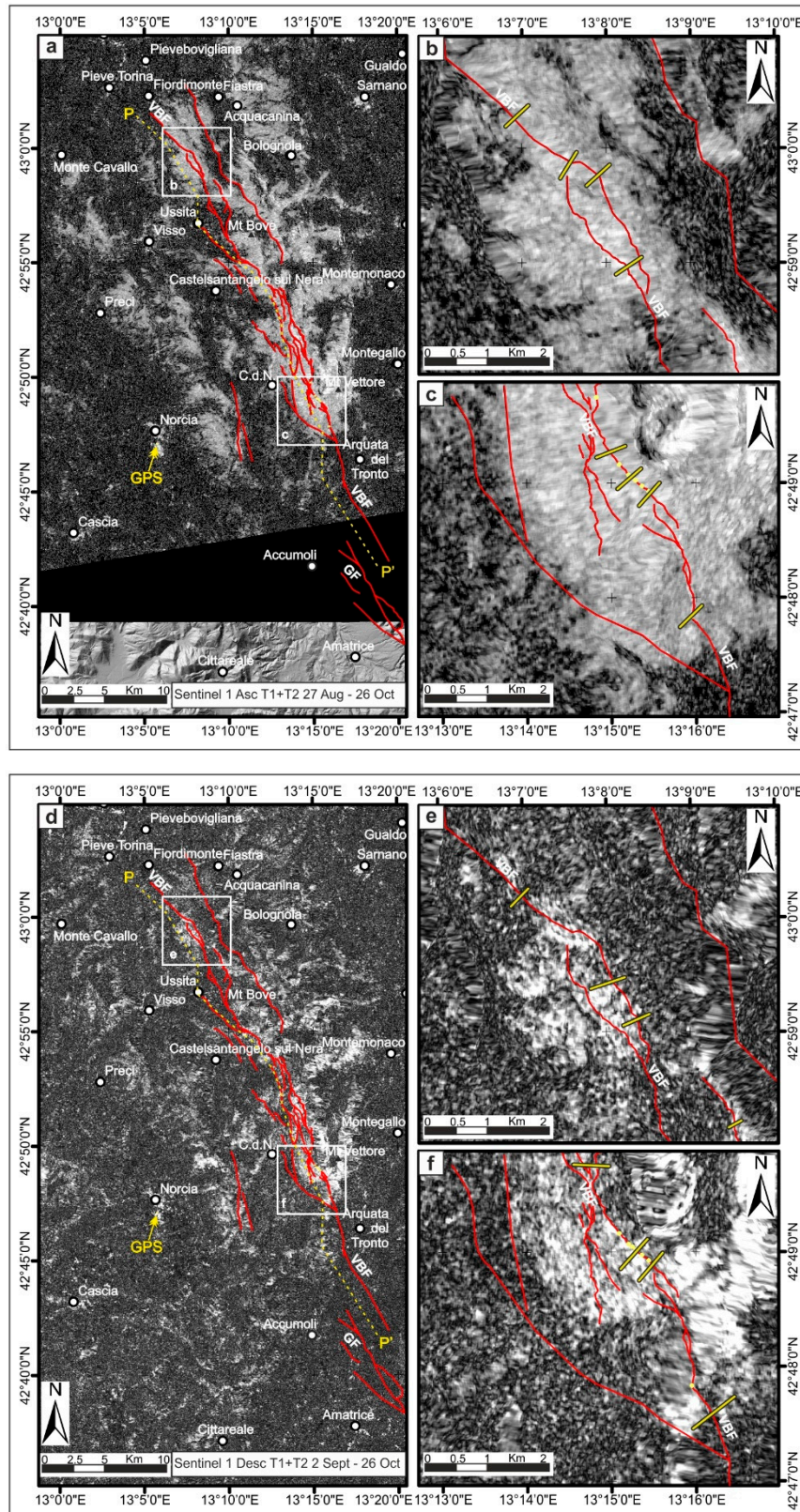


**Supplementary Figure S3g**

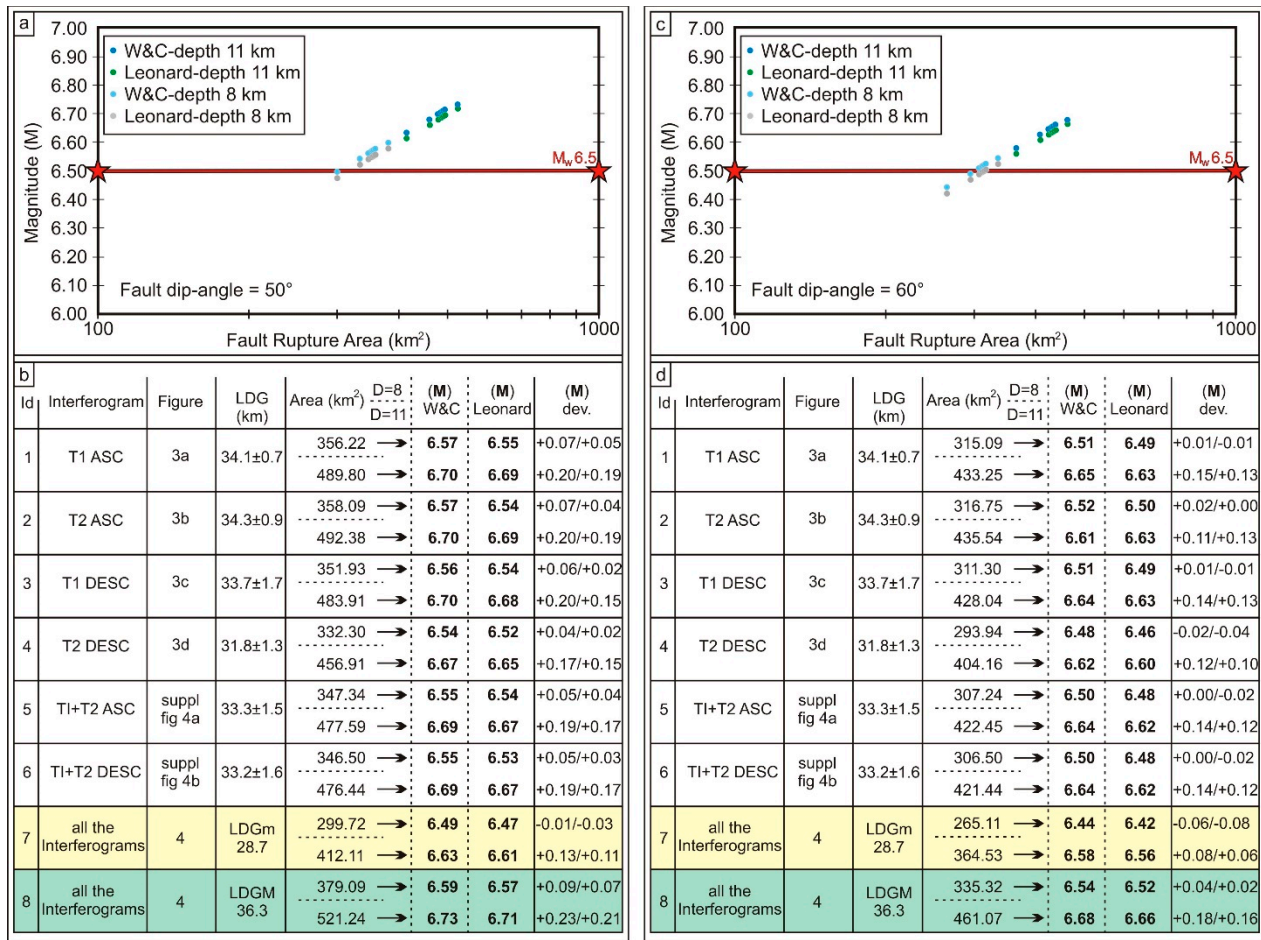
**Figure S3.** Additional field evidence of the intra-sequence (from 24 August to 29 October, 2016) slip deformations along the Mt Vettore–Mt Bove Fault (VBF).

Photographs taken at the survey sites reported in Figure 2a, showing the composite free faces due to different exhumation episodes during the 2016 seismic sequence. Three bands produced by different periods of exposure of the unearthed rocks. (a) Upper band showing the coseismic slip caused by the 24 August,  $M_w$  6.0 foreshock. (b) Intermediate band showing intra-sequence, slip between 24 August and 29 October 2016. (c) Lower (and thicker) band showing coseismic deformation caused by the  $M_w$  6.5 mainshock. Photographs taken on 2 July 2017. Field mapping performed on 27 and 28 of October 2016, showed that this segment of the VBF was not reactivated at the surface by the 26 October,  $M_w$  5.9 earthquake.

Photographs (a), (e), (f) and (g), showing permanent strain markers drawn to record the position of the topography cut-off line on the VBF hanging wall at different dates.



**Supplementary Figure S4.** Coherence map across the same areas shown in Figure 5 (Sentinel1 Ascending orbit 117=a–c) and Figure 6 (Sentinel1 Descending orbit 22=d–f). White regions locate the areas with maximum (~1) coherence. The precise trace of the Profile P-P', to which the graphs of Fig. 7c refer, is also drawn (yellow dotted line).



**Supplementary Figure S5.** Earthquake magnitude estimates from Length of the Deforming Ground (LDG). Plots (a, c) and Tables (b, d) show estimates for the earthquake magnitude  $M_w$  obtained from the LDG measured on the interferograms shown in Figure 3 a–d and Figure 4 and the  $LGD_M$  and  $LGD_m$  values assessed as reported in Section 2.3.  $M_w$  was calculated adopting the scaling relationships proposed by [2] and [3], and using Surface Rupture Length,  $SRL = LGD$ , and two epicentre depths,  $D = 8$  km and  $D = 11$  km [4,5]. In the plots, the red lines show the 30 October  $M_w$  6.5 mainshock. In the Tables, the rightmost column lists deviations of the estimated magnitude values from  $M_w$  6.5 of the mainshock, which are all less than 0.25.

**References for Supplementary Figures**

- Cheloni, D., et al., Geodetic Model of the Central Italy earthquake sequence inferred from InSAR and GPS data. *Geophys. Res. Lett.* 2017, 44, doi:10. 1002/2017GL073580.
- Wells, D., L. and Coppersmith, J. New empirical relationships among magnitude, rupture length, rupture width, rupture area, and surface displacement. *Bull. Seism. Soc. Am.* 1994, 84(4), 974–1002.
- Leonard, M. Earthquake fault scaling: self consistent relating of rupture length, width, average displacement and moment release. *Seism. Soc. Am. Bull.* 2010, 100(5A), 1971–1988, doi:10. 1785/0120120249.
- Lavecchia, G., et al. Ground deformation and source geometry of the August 24, 2016 Amatrice earthquake (Central Italy) investigated through analytical and numerical modeling of DInSAR measurements and structural-geological data. *Geophys. Res. Lett.* 2016, 43, 12, 389–12, 398, doi:10. 1002/2016GL071723.
- Michele M., et al. The Amatrice 2016 seismic sequence: a preliminary look at the mainshock and aftershocks distribution. *Annals Geophy.* 2016, 59, Fast Track 5, doi:10. 4401/ag-7227.

**Supplementary methods 1**

**DInSAR processing steps**

Here, we list the DInSAR processing steps that were used to prepare the interferograms used in the work exploiting the European Space Agency (ESA) Sentinel Application Platform (SNAP). For computation, we selected the parameters

suggested by the ESA SNAP, with some fine-tuning.

#### Step 1: Sentinel-1 Images TOPSAR Enhanced-Spectral-Diversity co-registration

This step co-registers two SAR images using information on the image orbits and a Digital Elevation Model (DEM). The quality of the co-registration increased [1] using the Enhanced Spectral Diversity algorithm and the following parameters:

- Registration Window Width = 1024
- Registration Windows Height = 1024
- Search Window Accuracy in Azimuth Direction = 32
- Search Window Accuracy in Range Direction = 32
- Window Oversampling Factor = 256
- Cross-correlation Threshold = 0.1
- Coherence Threshold for Outlier Removal = 0.15
- Number of Windows per Overlap for ESD = 10

#### Step 2: Sentinel-1 TOPSAR Deburst and Merge

First, bursts in each of the three sub-swath IW SLC images are “deburst” (i.e., joined). Next, the three sub-swaths are merged into a single swath. No input parameter is required.

#### Step 3: Interferogram production

The complex interferogram is computed including subtraction of the flat-Earth reference phase, based on the following parameters:

- Degree of flat-Earth polynomial = 5
- Number of flat-Earth estimation points = 601
- Orbit Interpolation degree = 3

Coherence estimation is obtained using square pixels having the following:

- Coherence Range Window Size = 10
- Coherence Azimuth Window Size = 3

#### Step 4: Optional multi-looking

Multi-looking is executed on the real in-phase (I) and quadrature (Q) components of the complex number obtained during Step 3, using the following parameters:

- Number of Range Looks = 10
- Number of Azimuth Looks = 3

to obtain a square pixel of approximately  $38.5 \times 38.5$  m.

We calculated the phase using the phase function available in the band map, and the coherence using the coherence estimation module with parameters consistent to those selected for number of looks. The step was executed to facilitate the phase unwrapping process (see Step 7).

#### Step 5: Topographic phase removal

We removed the topographic phase using the Shuttle Radar Topography Mission, SRTM 1-Sec HTG DEM, using the following parameters:

- Orbit Interpolation Degree = 3
- Tile extension = 100

#### Step 6: Filtering

We used the [2] phase filtering to enhance the phase unwrapping accuracy using the following parameters:

- Adaptive Filter Exponent = 1
- FFT size = 64
- Window size = 3

### Step 7: Phase unwrapping

For phase unwrapping, we used SNAPHU, a Statistical-Cost, Network-Flow Algorithm for Phase Unwrapping proposed by [3]. We provide an example of an input parameter file used to unwrap one of the interferograms as follows.

```
# Configuration file for SNAPHU
# Created by SNAP software on: 09:18:12 09/06/2017
# Command to call snaphu:
# snaphu -f snaphu.conf Phase_ifg_srd_VV_02Oct2016_26Oct2016.snaphu.img 4751
# Unwrapping parameters #
  STATCOSTMODE          DEFO
  INITMETHOD            MCF
  VERBOSE               TRUE
# Input files #
  CORRFILE              coh_VV_02Oct2016_26Oct2016_slv1_02Oct2016.snaphu.img
# Output files #
  OUTFILE               UnwPhase_ifg_srd_VV_02Oct2016_26Oct2016.snaphu.img
  LOGFILE               snaphu.log
# File formats #
  INFILEFORMAT          FLOAT_DATA
  CORRFILEFORMAT        FLOAT_DATA
  OUTFILEFORMAT         FLOAT_DATA
# SAR and geometry parameters #
  TRANSMITMODE          REPEATPASS
  ORBITRADIUS           7070073.827
  EARTH_RADIUS          6368475.423
  LAMBDA                0.0554658
  BASELINE              98.548
  BASELINEANGLE_RAD    3.01
  NEARRANGE             847615.1297989
# Slant range and azimuth pixel spacing
  DR                   23.2956211
  DA                   140.4612171
# Single-look slant range and azimuth resolutions.
  RANGERES             2653030.6018487
  AZRES                245.861392
  NCORRLOOKS           23.8
# Tile control #
  NTILEROW             5
  NTILECOL              5
  ROWOVRLP             0
  COLOVRLP             0
  NPROC                8
  TILECOSTTHRESH       500
# End of SNAPHU configuration file
```

### References for Supplementary Method 1

1. Sheilber, R. & Moreira, A. Coregistration of Interferometric SAR Images Using Spectral Diversity. *IEEE Transactions on Geoscience and Remote Sensing* **38** (5), 2179–2191, doi:10.1109/36.868876 (2000)

2. Goldstein, R.M. and Werner, C.L. Radar interferogram filtering for geophysical applications. *Geophy. Res. Letters* **25**: 4035–4038, doi:10.1029/1998GL900033 (1998).
3. Chen, C.W. & Zebker, H.A. Phase unwrapping for large SAR interferograms: statistical segmentation and generalized network models. *IEEE Transactions on Geoscience and Remote Sensing* **40** (8), 1709–1719, doi:10.1109/TGRS.2002.802453 (2002).